



HAL
open science

Streamlined targeting of Amaryllidaceae alkaloids from the bulbs of *Crinum scillifolium* using spectrometric and taxonomically-informed scoring metabolite annotations

Amon Diane N'Tamon, Aboua Timothée Okpekon, Nicaise Bony, Guillaume Bernadat, Jean-François Gallard, Tapé Kouamé, Blandine Séon-Méniel, Karine Leblanc, Somia Rharrabti, Elisabeth Mouray, et al.

► To cite this version:

Amon Diane N'Tamon, Aboua Timothée Okpekon, Nicaise Bony, Guillaume Bernadat, Jean-François Gallard, et al.. Streamlined targeting of Amaryllidaceae alkaloids from the bulbs of *Crinum scillifolium* using spectrometric and taxonomically-informed scoring metabolite annotations. *Phytochemistry*, 2020, 179, pp.112485. 10.1016/j.phytochem.2020.112485 . mnhn-02977175

HAL Id: mnhn-02977175

<https://mnhn.hal.science/mnhn-02977175>

Submitted on 30 Aug 2022

HAL is a multi-disciplinary open access archive for the deposit and dissemination of scientific research documents, whether they are published or not. The documents may come from teaching and research institutions in France or abroad, or from public or private research centers.

L'archive ouverte pluridisciplinaire **HAL**, est destinée au dépôt et à la diffusion de documents scientifiques de niveau recherche, publiés ou non, émanant des établissements d'enseignement et de recherche français ou étrangers, des laboratoires publics ou privés.



Distributed under a Creative Commons Attribution - NonCommercial 4.0 International License

Streamlined targeting of Amaryllidaceae alkaloids from the bulbs of *Crinum scillifolium* using spectrometric and taxonomically-informed scoring metabolite annotations

Amon Diane N'Tamon,^{a,b} Aboua Timothée Okpekon,^c Nicaise F. Bony,^b Guillaume Bernadat,^b Jean-François Gallard,^d Tapé Kouamé,^{a,c} Blandine Séon-Méniel^a, Karine Leblanc^a, Somia Rharrabti^a, Elisabeth Mouray,^e Philippe Grellier,^e Michèle Ake,^b N'Cho Christophe Amin,^b Pierre Champy,^a Mehdi A. Beniddir,^{a,*} and Pierre Le Pogam^{a,**}

^a Université Paris-Saclay, CNRS, BioCIS, 92290, Châtenay-Malabry, France

^b Département de Chimie Analytique, Minérale et Générale, Technologie Alimentaire, UFR Sciences Pharmaceutiques et Biologiques, Univ. FHB, 06 B. P. 2256 Abidjan 06, Côte d'Ivoire

^c Laboratoire de Chimie Organique et de Substances Naturelles (LCOSN), UFR Sciences des Structures de la Matière et Technologie, Univ. FHB, 22 BP 582 Abidjan 22, Côte d'Ivoire

^d Institut de Chimie des Substances Naturelles, CNRS, ICSN UPR 2301, Université Paris-Saclay, 21 Avenue de la Terrasse, 91198 Gif-sur-Yvette, France

^e Muséum National d'Histoire Naturelle, Unité Molécules de Communication et Adaptation des Micro-organismes, UMR7245, CP54, 57 Rue Cuvier, 75005, Paris, France

* Corresponding author.

** Corresponding author.

E-mail addresses: mehdi.beniddir@universite.paris-saclay.fr (M. A. Beniddir), pierre.le-pogam-alluard@universite.paris-saclay.fr (P. Le Pogam)

Keywords: *Crinum scillifolium*, Amaryllidaceae, Alkaloids, Molecular Networking, In Silico Data Base.

Abstract

Four undescribed alkaloids have been isolated from the bulbs of the previously unstudied *Crinum scillifolium*. These compounds were targeted following a state-of-the-art molecular networking strategy comprising a dereplication against in silico databases and re-ranking of the candidate structures based on taxonomically informed scoring. The unreported structures span across a variety of Amaryllidaceae alkaloids appendages. Their structures were unambiguously elucidated by thorough interpretation of their HRESIMS and 1D and 2D NMR data, and comparison to literature data. DFT-NMR calculations were performed to support the determined relative configurations of scillitazettine and scilli-*N*-desmethylpretazettine and their absolute configurations were mitigated by comparison between experimental and theoretically calculated ECD spectra. The lack of a methyl group on the nitrogen atom in the structure of scilli-*N*-desmethylpretazettine series is highly unusual in the pretazettine/tazettine series but the most original structural feature in it lies in its 11 α disposed hydrogen, which is new to pretazettines. The antiplasmodial as well as the cytotoxic activities against the human colon cancer cell line HCT116 were evaluated, revealing mild to null activities.

1. Introduction

Amaryllidaceae plants are divided into 85 genera and encompass more than 1100 species that are widely spread throughout both tropical and warm temperate regions of the world (Jin and Yao, 2019). From a chemical viewpoint, this family is mostly renowned for sheltering more than 600 of the so-called Amaryllidaceae alkaloids, a collection of unique and structurally diverse tyrosine and phenylalanine-derived specialized metabolites (Hotchandani and Desgagne-Penix, 2017; Singh and Desgagné-Penix, 2017). This specific chemodiversity is endowed with varied and significant pharmacological traits, the most salient of which include the cytotoxic narciclasine (Dumont et al., 2007), the anti-parasitic haemanthamine (Cedrón et al., 2012), the anti-viral lycorine (Zou et al., 2009) and the anti acetylcholinesterase galanthamine (Thomsen and Kewitz, 1990; López et al., 2002). Intense phytochemical investigation campaigns were geared towards the isolation of undescribed alkaloids from this privileged taxa throughout the last decades, resulting in the isolation and structure elucidation of 44 alkaloids during the sole two year-timeframe between 2015 and 2017 (Jin and Yao, 2019). Notwithstanding their rather low molecular weights, the structure elucidation of these polycyclic compounds, often depauperate in H atoms, is globally challenging, accounting for the elevated number of such structures only being partially elucidated (Buckingham et al., 2010). Fueled by numerous ethnopharmacological claims (Fennell and Van Staden, 2001), *Crinum* spp. chemistry was deeply dug so that this genus, sustained by more than 160 species, afforded so far *ca.* 200 different alkaloids spanning across most Amaryllidaceae alkaloid frameworks. Nevertheless, as of 2020, some species still have to be studied from a chemical perspective including *Crinum scillifolium* A. Chev. that is encountered in periodically flooded forest area throughout Liberia and Ivory Coast. Like many plants pertaining to the *Crinum* genus (Refaat et al., 2013, 2012a, 2012b), *C. scillifolium* is being used in folk medicine for various ailments, and these data are partly

corroborated by in vivo studies from crude extracts, adding further interest in the chemical investigation of this species (Koua Kadio Brou et al., 2018, 2017a, 2017b). This report outlines the molecular networking-guided isolation, structure elucidation, and evaluation of antiplasmodial and cytotoxic activities of four unreported alkaloids of various structural series, along with the previously isolated asiaticumine A (Sun et al., 2009), 4'-*O,N*-dimethylnorbelladine (Pilar Vazquez Tato et al., 1988), vittatine (Frahm et al., 1985; Pabuçcuoglu et al., 1989), hippadine (Ali et al., 1981), lycorine (Evidente et al., 1983), 4'-*O*-methylnorbelladine (Eichhorn et al., 1998), sternbergine (Evidente et al., 1984), and isotazettinol (Ünver et al., 1999) from this species. To assist further phytochemical investigations involving Amaryllidaceae plants, the MS/MS data related to all isolated molecules were uploaded to the GNPS repositories (Wang et al., 2016).

2. Results and discussion

To get a first insight into the so-far unstudied specialized metabolite content of *C. scillifolium*, the alkaloid extract of the bulbs and the five fractions obtained from the first chromatographic fractionation were profiled by HPLC-HRMS/MS. These data were subsequently preprocessed and organized using the feature-based molecular networking workflow (Nothias et al., 2019). As already pointed out, the success of this dereplication strategy highly depends on the quality and availability of MS/MS data, accounting for the stern efforts of natural product researchers being geared towards the upload of reference mass spectrometric data related to their favorite structural series (Fox Ramos et al., 2019b; Olivier-Jimenez et al., 2019; Wang et al., 2016). The annotation of the generated molecular network (Fig. 1) against the GNPS spectral libraries did not return a single tentative hit corresponding to an Amaryllidaceae alkaloid, despite revealing a substantial number of even-numbered nodes, presumably related to an array of different alkaloids. To extend the degree of spectrometric annotation when experimental tandem mass spectrometric are scarce or absent

(Fox Ramos et al., 2019a), an elegant strategy was designed by Allard et al. to enable the dereplication of experimental MS/MS data against CFM-ID-predicted (Allen et al., 2015) mass spectrometric data for 200.000 natural products entries of the Universal Natural Products Dictionary (Allard et al., 2016). The confidence in structure assignment can be enhanced by integrating further degrees of functional annotations such as the taxonomic position of the investigated material (Fox Ramos et al., 2019a). For this purpose, a recently implemented script by Allard and co-workers offers the opportunity to complement the score obtained between experimental spectral data and the output of computational metabolite annotation tools such as ISDB (In Silico Data Base) (Rutz et al., 2019). As an illustration of this annotation strategy, the tagging of a specific node is displayed both before and after this taxonomic re-ranking in Fig. S2, Supporting Information. This refined annotation strategy provided some entry points in the generated molecular network (Fig. 1) and LC-DAD-MS analyses monitoring defined a shortlist of compounds seemingly amenable to isolation in sufficient amounts for full structure elucidation. These targeted structures tightly clustered with tentatively annotated nodes (**2**, m/z 330.1303 and **3**, m/z 314.1351) or showed up as self-loops (**1**, m/z 360.1503 and **4**, m/z 304.1488). Accordingly, compounds **1–4** could be isolated following repeated chromatographic fractionations (Fig. 2).

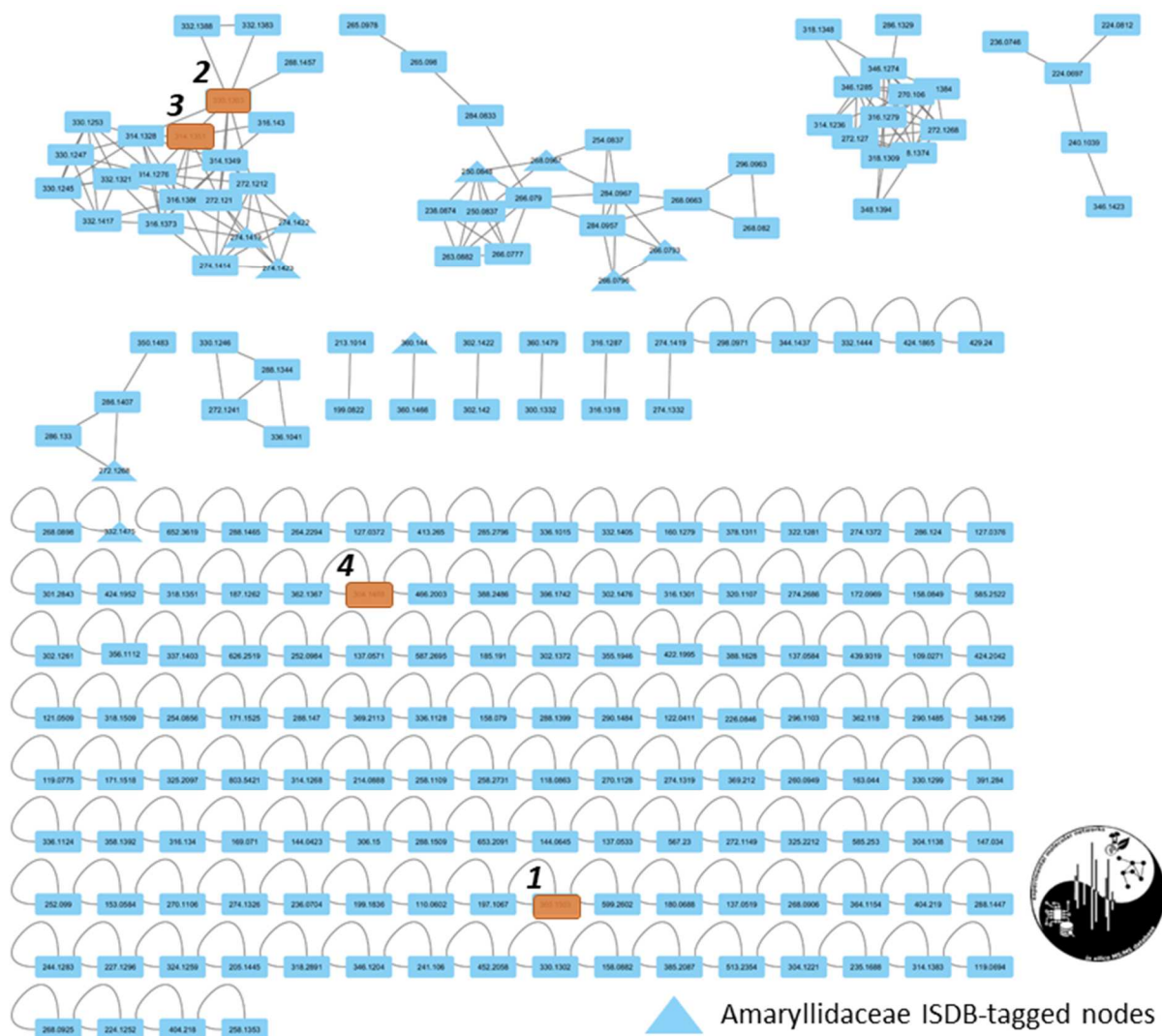


Fig. 1. Overall molecular network obtained from MZmine2-processed HPLC-MS² data of *C. scillifolium* bulbs crude alkaloid extract and first chromatographic fractions. Triangle-shaped nodes are tentatively-tagged against ISDB and benefit from a taxonomical re-ranking of the tentative candidates (their structures are provided in Fig. S1, Supporting Information). Nodes highlighted in orange correspond to the targeted structures (**1-4**) in the phytochemical workflow.

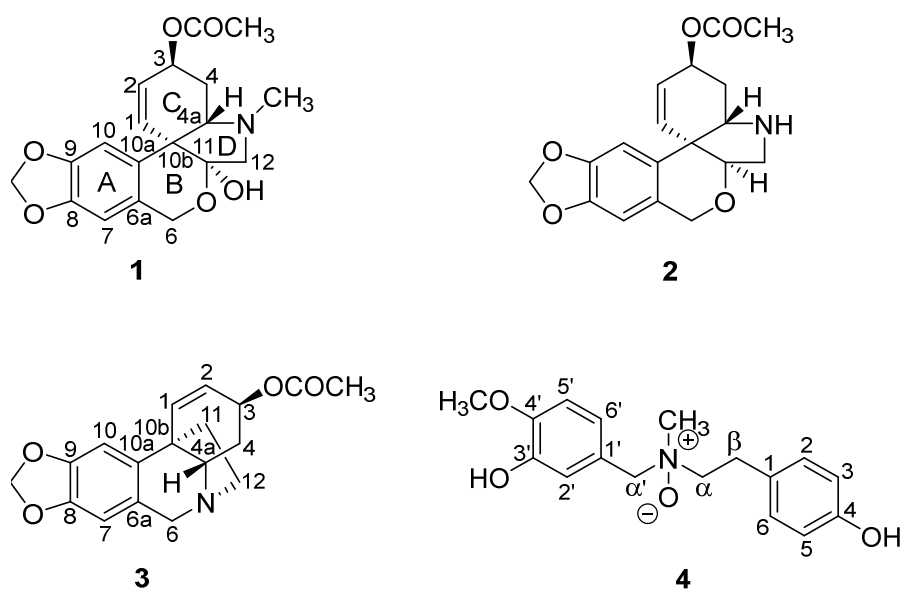


Fig. 2. Structures of compounds **1–4**.

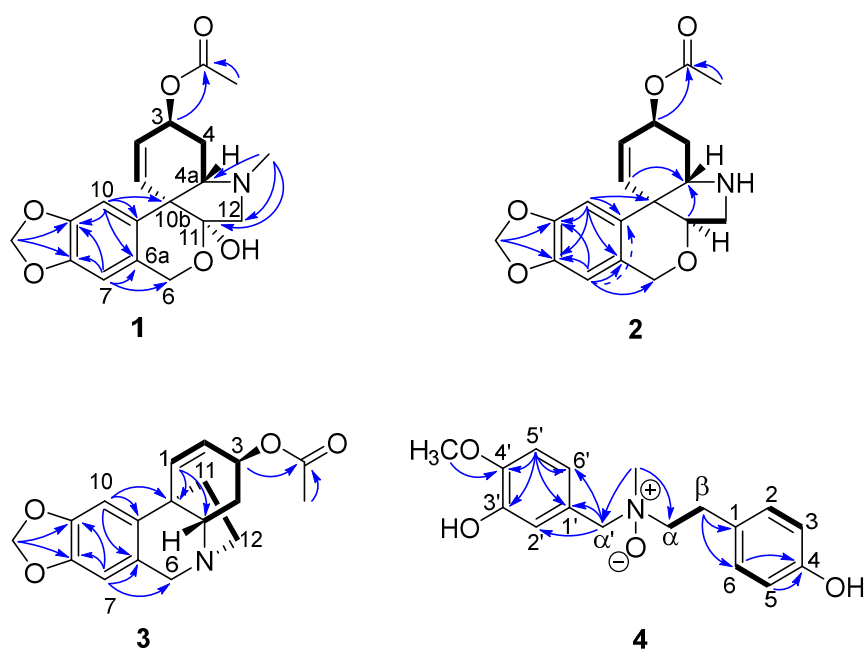


Fig. 3. Key COSY and HMBC correlations of compounds **1–4**.

Compound **1** was obtained as an amorphous solid with a molecular formula of $C_{19}H_{21}NO_6$, established by the HRESIMS ion at m/z 360.1448 (calcd for $C_{19}H_{22}NO_6$, 360.14416). The preliminary investigation of both the 1H NMR spectrum showed two singlets at δ_H 6.75 (H-7) and 6.58 (H-10) and a methylene group at δ_H 5.79 (2H, s), that was diagnostic of the joined

1,3-dioxolane cycle, as often encountered within Amaryllidaceae alkaloids. The ^1H NMR spectrum also comprised a doublet of triplets at δ_{H} 5.75 ($J = 10.5, 1.6$ Hz) and a broad doublet at δ_{H} 5.84 ($J = 10.5$ Hz), diagnostic of olefinic protons, a broad doublet of doublet of doublets at δ_{H} 5.62 ($J = 9.5, 6.8, 1.6$ Hz) corresponding to the adjacent oxygenated methine, the connectivities of which are outlined throughout COSY analyses (Fig. 3). The thorough analysis of the ^1H NMR spectrum, along with COSY correlations, determined H-3 as the X component of an ABMX spin system, where the AB are the two diastereotopic methylene signals arising as a multiplet at δ_{H} 2.29 and a doublet of doublet of doublets at δ_{H} 1.74 ($J = 13.5, 9.5, 2.2$ Hz), and the M part is a proton at δ_{H} 2.94. These NMR landmarks are evocative of the C cycle of tazettine-type alkaloids (Masi et al., 2015). The signals corresponding to a $N\text{-CH}_3$ moiety resonating at δ_{H} 2.46, an AB system corresponding to the diastereotopic methylenic protons of C-12, and a last AB doublet due to an oxygenated diastereotopic methylene at δ_{H} 4.63 and 4.98 were in line with a tazettine-type scaffold as supported by the HMBC correlations, outlined in Fig. 3, that led to determine the planar structure, namely scillitazettine, as shown in Fig. 2. Inferring the half-chair conformation of the C cycle, the magnitude of the vicinal coupling constant between H-3 and H-4B (9.5 Hz) and H-3 and H-4A (6.8 Hz) hinted the α - and β -pseudoaxial orientations of H-3 and H-4B, and ascribing the α -pseudoequatorial orientation of H-4A, in full agreement with the spectroscopic data of the structurally-related compound jonquiline (Masi et al., 2015). Then, the value of 2.2 Hz determined between H-4B and H-4a established the β -pseudoequatorial disposition of H-4a, consistently with the consensual orientation of this proton by regards to biosynthetic considerations (Jin and Yao, 2019). The DFT-optimized geometry of the lowest-energy conformer of **1** revealed that the structural information conveyed by NOESY correlations should be interpreted very cautiously, owing to the β -pseudoequatorial disposition of H-4a that displays a roughly similar interatomic distance with both protons of the diastereotopic

methylenic pair H-4A and H-4B (Fig. S15, Supporting Information). In these conditions, it appeared tricky to draw any conclusion as to synfacial or antifacial dispositions of H-3 and H-4a based on their NOE crosspeaks to H₂-4. Seeking independent evidence to support the preferred configuration detailed above, DFT-NMR calculations were undertaken to determine the correct diastereoisomer among the candidates differing in the configuration of C-3 but also of C-11 which is not assignable based on NMR data. The subsequent DP4 probability method demonstrated the structural equivalence of **1** with diastereoisomer **1A** with 90.9% probability (Fig. S14, Supporting Information).

Gratifyingly, the calculated coupling constants were in excellent agreement with our experimental values (Fig. S15, Supporting Information). The ECD spectrum of **1**, displaying a positive/negative arrangement at the indicated wavelengths, was highly reminiscent of a tazettine arrangement (viz. *cis* B/D cycles) (Wagner et al., 1996; Pham et al., 1999). These empirical correlations were however sometimeproved to fail, leading us to question the reliability of these rules (Vergura et al., 2018). The (3*S*, 11*S*) absolute configuration of **1** was subsequently assigned based on comparison between the calculated (TDDFT) and experimental electronic circular dichroism (ECD) spectra (Fig. 4). These spectroscopic data defined **1** as the acetyl derivative of 3-*O*-demethyltazettine (Pham et al., 1999), namely scillitazettine, as indicated in Fig. 2.

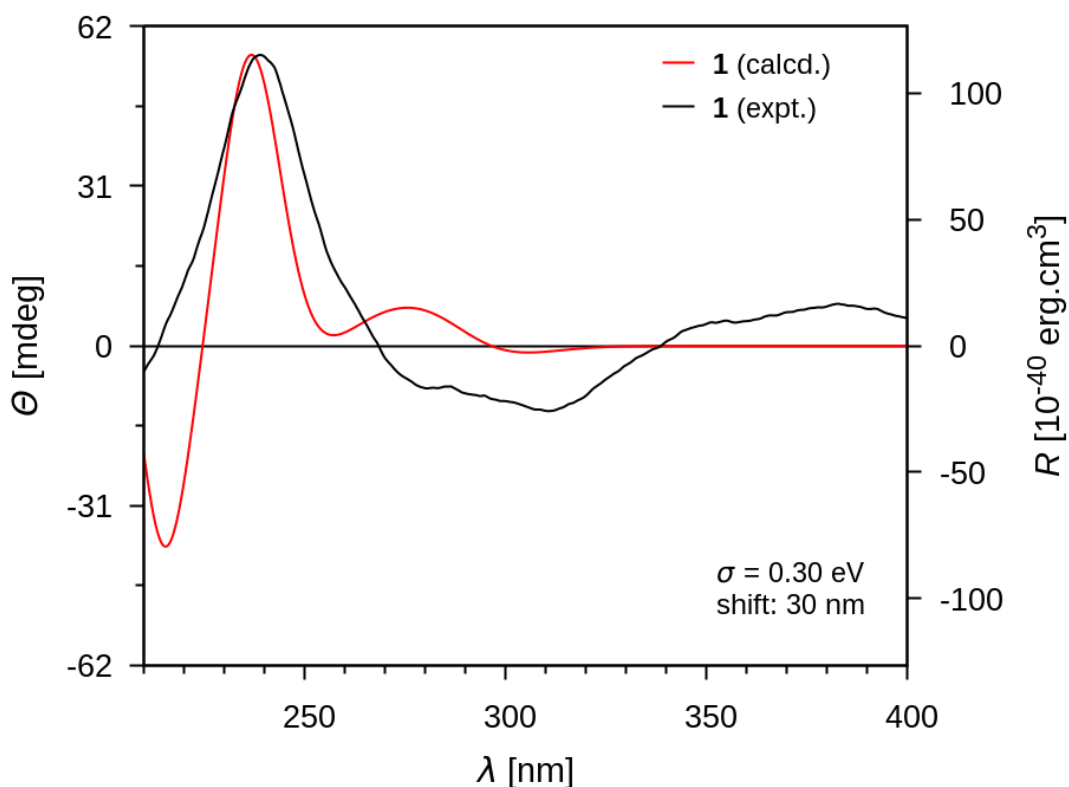


Fig. 4. Comparison of the experimental ECD spectrum of **1** and calculated ECD spectrum for the (3*S*, 4*aS*, 10*bS*, 11*S*) enantiomer.

Compound **2** was obtained as a white amorphous solid. The ^{13}C NMR and (+)-HRESIMS data established a molecular formula of $\text{C}_{18}\text{H}_{19}\text{NO}_5$, differing from compound **1** by the loss of a methyl group and of an OH moiety. Accordingly, the ^1H and ^{13}C NMR data exhibited many signals analogous to those observed in **1**, *i. e.* NMR landmarks related to the methylenedioxyphenylene core and the oxygenated diastereotopic methylene signals of cycle B, the ABMX spin system related to cycle C, with the main salient differences being the disappearance of the N- CH_3 signal and the arising of an oxygenated methine proton resonating at δ_{H} 4.12 (1H, dd, $J = 6.0, 1.0$ Hz)/ δ_{C} 80.2 that seemingly replaced the hemiketalic carbon at C-11, consistent with spectroscopic data of pretazettine derivatives (Cabezas et al., 2003; Elgorashi et al., 1999). This assumption was validated by this proton being the X component of an ABX spin system comprising a diastereotopic methylene group (δ_{H} 3.73

(1H, dd, $J = 13.0, 6.0$ Hz) and δ_{H} 3.66 (1H, dd, $J = 13.0, 1.0$ Hz)). The magnitude of the coupling constant values $J_{11/12\alpha}$ and $J_{11/12\beta}$ can be used to assign C-11 configuration (Kobayashi et al., 1980). Regarding **2**, the small value of these parameters hinted the α -orientation of H-11 (Kobayashi et al., 1980), which was further backed up by the NOE cross-peak between H-1 and H-11. Here again, the DFT-optimized geometries of lowest-energy conformers for this tentative structure of **2** accounted for the poor degree of information that could be retrieved from the NOESY spectrum, by regards to the nearly identical interatomic distances between H-3 and both diastereotopic methylenic protons H₂-4 (Fig. S27, Supporting Information). The relative configuration of **2** was thus mainly based on coupling constant analyses, and comparison with former literature reports. The small magnitude of the vicinal coupling constants between H-3 and both diastereotopic methylenic protons H₂-4 and the large coupling constant of H-4a with H-4A ($J = 13.4$ Hz) hinted an α -orientation of H-3 (Brine et al., 2002; Zhan et al., 2016; Wang et al., 2018), which was also supported by the NOE crosspeak between H-3 and H-4A. To get an independent validation of this determined relative configuration, DFT-NMR calculations were carried out for the four different diastereoisomeric candidates at C-3 and C-11. Accordingly, DP4 calculation resulted in the prediction of the **2A** diastereoisomer with 81.0 % probability (Fig. S26, Supporting Information). The absolute configuration of **2** was finally assigned based on a comparison between the calculated (TDDFT) and experimental circular dichroism spectra (Fig. 5). Compound **2**, namely scilli-*N*-desmethylpretazettine, pertains to a rare structural class as it extends the small phytochemical class of *N*-desmethylpretazettine derivatives, third to those which were simultaneously reported from *Crinum bulbispermum* (Elgorashi et al., 1999). From a stereochemical viewpoint, although a full absolute configuration is being proposed by the authors, their claims are not supported by any convincing spectroscopic feature since vicinal coupling constant values are partly being described and are not discussed and the ECD

spectrum was not even recorded (Elgorashi et al., 1999). A further originality in the structure of **2** is the α -orientation of H-11, here first reported in the pretazettine/tazettine series (Berkov et al., 2020). A single pretazettine was formerly proposed to have a 11α oriented hydrogen proton but the determination of this compound, namely 11-desoxy-12-methoxycrivelline, only relied on GC-MS data, rendering its structure highly dubious (Bokov et al., 2016; Berkov et al., 2020).

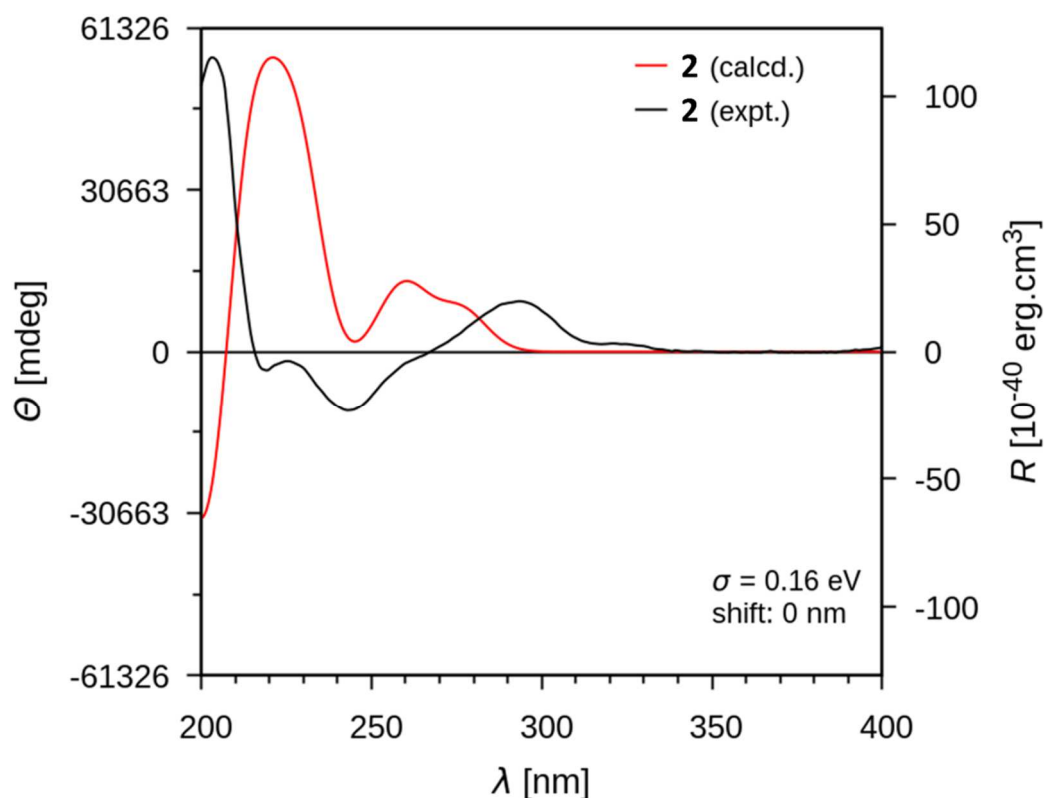


Fig. 5. Comparison of the experimental ECD spectra of **2** and calculated ECD spectra for stereoisomer of **2** shown in Fig. 2.

Compound **3** was isolated as a white amorphous solid. Its molecular formula was deduced to be $C_{18}H_{19}NO_4$ by the (+)-HRESIMS and the ^{13}C NMR data. The 1H NMR spectrum revealed analogous NMR landmarks for a methylenedioxyphenylene core including the methylenedioxy protons at δ_H 5.91 (2H, s), and the *para*-disposed aromatic protons at δ_H 6.61 (1H, s), and 6.97 (1H, s), olefinic protons at δ_H 6.77 (1H, d, $J = 10.0$ Hz) and 5.94 (1H, dd, $J =$

10.0, 5.1 Hz), the ABMX spin system comprising a diastereotopic methylene pair at δ_{H} 2.04 and 2.07, an acetyl-methyl linked oxygenated methine at δ_{H} 5.33 (1H, td, $J = 5.1, 4.7$ Hz), and an heteroatom-bearing methine (mandatorily the nitrogen atom owing to molecular formula requirements). A second spin system comprised two pairs of diastereotopic methylene protons resonating at δ_{H} 2.07 and 2.25 and at δ_{H} 3.12 and 3.52, these later being diagnostic of their *N*-bearing status, and finally a second pair of *N*-linked diastereotopic methylene resonating at δ_{H} 3.99 and 4.51. Altogether, these spectroscopic features defined a planar crinane/haemanthamine-type scaffold, as further supported by long-range heteronuclear correlations outlined in Fig. 3. The magnitude of the coupling constant values between the olefinic protons (H-1 and H-2) and H-3 was used to bisect the relative orientation of this proton relatively to the ethano-bridge C-11/C-12. The currently observed coupling constants of the olefinic protons ($J_{1-3} = 0$ Hz; $J_{2-3} = 5.1$ Hz) were congruent with a *trans* orientation of the acetyl methyl substituent at C-3 to the two-carbon bridge (Abdel-Halim et al., 2004; Bastida et al., 1990, 2006). The absolute configuration of **3** was further established by circular dichroism. As formerly reported for various haemanthamine derivatives, the positive Cotton effect around 290 nm, and the negative Cotton effect around 250 nm were diagnostic of an alkaloid with the ethano bridge in an α -orientation (Abdel-Halim et al., 2004; Herrera et al., 2001; Wagner et al., 1996). Altogether, these spectroscopic data identified **3** as 3-*O*-acetylvittatine. Noteworthy, 3-*O*-acetylvittatine was tentatively identified from several Amaryllidaceae plants (Tallini et al., 2017; Torras-Claveria et al., 2010). Yet, as far as can be ascertained, all structural reports related to this compound are based on mass spectrometric fragmentation patterns following gas- or liquid- chromatography and it seems that this molecule was not isolated previously.

Compound **4** was obtained as a white amorphous solid with a molecular formula of $\text{C}_{17}\text{H}_{21}\text{NO}_4$, established by the HRESIMS ion at m/z 304.1595 (calcd for $\text{C}_{17}\text{H}_{22}\text{NO}_4$,

304.15433). The ^1H NMR spectrum of **4** revealed an AA'BB' spin system comprising two pairs of two-proton doublets at δ_{H} 7.11 (2H, d, $J = 8.2$ Hz) and 6.76 (2H, d, $J = 8.2$ Hz), a set of ABX system aromatic protons at δ_{H} 7.04 (1H, dd, $J = 8.3, 2.4$ Hz), 7.07 (1H, d, $J = 2.4$ Hz), and 7.01 (1H, d, $J = 8.3$ Hz), three poorly-resolved methylene signals at δ_{H} 3.15, 3.57 and 4.57 (with these two latter being heteroatom-bonded owing to their downfield-shifted carbon signals at δ_{C} 29.6, 69.3 and 73.2), a methoxy group at δ_{H} 3.90 (3H, s), and a low-field shifted nitrogen-located methyl group at δ_{H} 3.22 (3H, s) (Table 2). These NMR data were evocative of the benzyl-1-phenylethylamine appendage of norbelladine derivatives (Jin and Yao, 2019; Zetta et al., 1973). This hypothesis was validated through the HMBC correlations from the *N*-methyl group at δ_{H} 3.22 to both the carbons at δ_{C} 69.3 (C- α) and at δ_{C} 73.2 (C- α'). The downfield chemical shift of the protons and carbons *alpha* to the nitrogen compared to related norbelladine derivatives suggested the quaternary nature of the nitrogen atom, in line with molecular formula requirements that needed the introduction of an additional oxygen atom (Suau et al., 1988; Nair et al., 2005; Fox Ramos et al., 2017). This structure was ultimately validated by comparison against the NMR data of the non *N*-oxide version of this molecule (Pilar Vazquez Tato et al., 1988), *i.e.* the co-isolated 4'-*O,N*-dimethylnorbelladine, and was therefore named 4'-*O,N*-dimethylnorbelladine *N*-oxide. Both the null optical activity and the lack of any Cotton effect determined the racemic status of **4**.

Table 1.¹H (400 MHz) and ¹³C NMR (100 MHz) data for **1–3** in CD₃OD

	1^a		2^b		3^b	
position	δ_{H} (<i>J</i> in Hz)	δ_{C}	δ_{H} (<i>J</i> in Hz)	δ_{C}	δ_{H} (<i>J</i> in Hz)	δ_{C}
1	5.75, td (10.5, 1.6)	132.3	6.59, d (10.1)	130.1	6.77, d (10.0)	134.5
2	5.84, br d (10.5)	130.8	6.26, dd (10.1, 5.1)	129.1	5.94, dd (10.0, 5.1)	124.8
3	5.62, ddd (9.5, 6.8, 1.6)	69.2	5.39, td (5.1, 4.6)	67.6	5.33, td (5.1, 4.7)	67.3
4	α 2.29, m	27.2	α 2.52, ddd (15.1, 13.6, 4.3)	29.3	2.07, ddd (10.1, 5.1, 1.1)	29.7
	β 1.74 ddd (13.5, 9.5, 2.2)		β 2.09, m, ov.		2.04, m	
4a	2.94, m	72.9	3.67, dd (13.6, 2.7)	64.6	3.52, dd (12.1, 3.9)	64.8
6	4.63, d (14.8)	63.5	4.07, d (16.0)	60.7	3.99, d (16.0)	61.9
	4.98 d (14.8)		4.58, d (16.0)		4.51, d (16.0)	
6a	-	128.2	-	135.4	-	136.5
7	6.75, s	110.6	6.67, s	108.2	6.61, s	108.0
8	-	148.7	-	148.7	-	147.8
9	-	149.0	-	148.2	-	148.3

10	6.58, s	106.0	7.02, s	104.5	6.97, s	104.0
10a	-	128.5	-	124.6	-	125.9
10b	-	51.6	-	51.5	-	45.7
11	-	103.2	4.12, dd (6.0, 1.0)	80.2	2.07, m	44.0
	-		-		2.25, m	
12	2.74, d (10.9)	66.3	3.66, dd (13.0, 1.0)	63.2	3.12, m	53.8
	3.32, d (10.9)		3.73, dd (13.0, 6.0)		3.52, m	
OCH ₂ O	5.79, s	102.9	5.97, s	102.6	5.91, s	102.4
NCH ₃	2.46, s	43.9	-	-	-	
OCOCH ₃	2.13, s	21.9	2.09, s	21.0	1.99, s	20.9
OC <u>O</u> CH ₃	-	173.4	-	172.2	-	171.1

^a Recorded at 400/100 MHz, ^b Recorded at 600/150 MHz.

Table 2.¹H and ¹³C NMR Spectroscopic Data (400/100 MHz, CD₃OD) for **4**.

4		
position	δ_{H} (<i>J</i> in Hz)	δ_{C}
1	-	127.8
2/6	7.11, d, (8.2)	130.6
3/5	6.76, d, (8.2)	116.2
4	-	157.8
α	3.57, br s	69.3
β	3.15, br s	29.6
1'	-	122.0
2'	7.07, d (2.4)	120.2
3'	-	147.8
4'	-	150.5
5'	7.01, d, (8.3)	112.5
6'	7.04, dd, (8.3, 2.4)	125.4
α'	4.57, s	73.2
4'-OCH ₃	3.90, s	56.4
<i>N</i> -CH ₃	3.22	53.1

The occurrence of acetyl substituents is common in Amaryllidaceae alkaloids (Berkov et al., 2020). However, since the alkaloidic fractionation undertaken in this investigation comprised ethyl acetate as the organic phase, it was important to detect these compounds in an extract which did not imply ethyl acetate to demonstrate the genuine natural origin of compounds **1-3**. Fortunately, these compounds could also be detected in the crude ethanolic extract, ruling out the possibility that these compounds could only represent extraction artifacts (Fig. S46-S48, Supporting Information).

The specialized metabolites responsible for the numerous ethnopharmacological claims related to Amaryllidaceae plants have been under intense scrutiny throughout the last decades, especially their cytotoxic activity (Evidente and Kornienko, 2009) and their antiplasmodial properties (Nair and van Staden, 2019a). This prompted us to undertake the assessment of the antiparasitic activity of the isolated metabolites against the chloroquine-resistant strain of *Plasmodium falciparum* FcB1. Among the undescribed compounds (**1** and **2**) assayed for their antiplasmodial activity, compound **2** exerted the most significant activity (Table 4). The evaluated known compounds showed weak to moderate antiparasitic activity. The most active compound among the evaluated substances in our assays, lycorine, was formerly reported to exert strong antiplasmodial activity on some strains but was also reported inactive sometimes depending on the evaluated strain, and it seems that the FcB1 strain was not evaluated before (Nair and van Staden, 2019). Consistent with our current findings, sternbergine was found less active than lycorine although displaying slightly lower IC₅₀ values on formerly tested *P. falciparum* strains (Campbell et al., 2000). The modest antiplasmodial activity of the tazettine/pretazettine derivatives included in this study is in line with former activities obtained with the five derivatives of this family described so far that reported on null activities or at best, mild activity (*ca.* 10 µM for tazettine on some strains) (Nair and van Staden, 2019b). Likewise, the members of the small group of norbelladines were only scarcely studied for their antiplasmodial activities, but here again, the modest activity is consistent with the null or at best marginal activities reported so far (Nair and van Staden, 2019a). The cytotoxic activity of the isolated molecules was evaluated against the human colon cancer cell line HCT116 at the concentrations of 10⁻⁵ M and 10⁻⁶ M. The poor recorded activities (Table S58, Supporting Information) deterred us from sharply calculating their IC₅₀ values, with only **2** having an IC₅₀ comprised in this range of concentrations.

Table 4. IC₅₀ values (µM) of the antiplasmodial activities of isolated compounds^a

compound	<i>P. falciparum</i> strain FcB1
----------	----------------------------------

1	77.0 ± 2.0
2	46.5 ± 2.0
isotazettinol	23.0 ± 3.0
lycorine	11.0 ± 0.0
sternbergine	26.0 ± 2.0
4'- <i>O</i> -methylnorbelladine	30.5 ± 5.0
asiaticumine A	42.0 ± 0.0
chloroquine (nM)	59.0 ± 8.0

^a Values are mean ± standard errors of three independent experiments.

3. Conclusion

In summary, four previously undescribed Amaryllidaceae alkaloids have been obtained from *Crinum scillifolium*, here first studied from a chemical viewpoint. These structures were pinpointed, and their isolation streamlined, based on a molecular networking workflow benefitting from a state-of-the-art annotation strategy, including dereplication against in silico database and subsequent taxonomic reweighting. Three of the isolated structures extended the diversity of minor classes of Amaryllidaceae alkaloids, *viz.* tazettine, pretazettine, and norbelladines. The relative and absolute configuration assignments benefitted from extensive spectroscopic evidence. The assistance of DFT-NMR calculations fully rationalized the observed coupling constants, which might assist the structure elucidation of further related derivatives. With compound **2**, this investigation notably reports on the first occurrence of a pretazettine having a 11 α oriented hydrogen. These molecules revealed mild antiplasmodial activities and did not exert significant cytotoxic effects.

4. Experimental section

4.1. General experimental procedures

Optical rotations were obtained at 25°C on a Polar 32 polarimeter. UV and ECD spectra were recorded at 25°C on a Jasco J-810 spectropolarimeter. The NMR spectra were recorded on a Bruker AM-300 (300 MHz), AM-400 (400 MHz), and AM-600 (600 MHz). NMR

spectrometers were calibrated using solvent residual signals as references. Analytical HPLC runs were carried out using an Agilent LC-MS system consisting of an Agilent 1260 Infinity HPLC hyphenated with an Agilent 6530 ESI-Q-TOF-MS operating in positive polarity. Silica 12 g Grace cartridges were used for flash chromatography using an Armen instrument spot liquid chromatography flash apparatus. Sunfire preparative C₁₈ column (150 x 4.6 mm, i. d. 5 µm, Waters) were used for preparative HPLC separations using a Waters Delta Prep consisting of a binary pump (Waters 2525) and a UV-visible diode array detector (190-600 nm, Waters 2996). The preparative TLC plates used for purification were glass backed (20x20cm) and normal phase silica plates (250 µm thickness) purchased from Macherey-Nagel (Düren, Germany). The preparative TLC runs were performed in presaturated development chambers in dedicated solvent systems. After having fully air-dried, silica was scrapped off the plate and the bands of interest were desorbed in MeOH three times (30 min each) under sonication.

4.2. Plant material

Crinum scillifolium whole plants were collected in the PK37 area of the « Autoroute du Nord » between Abidjan and Yamoussoukro (GPS N 5.5017210, E -4.243631) in May 2018. The botanical identification was performed at the Centre National de Floristique (CNF)- Université Félix Houphouët Boigny – Abidjan (Côte d’Ivoire). A voucher specimen (No. DNT-CS-2018) is kept at the herbarium of CNF.

4.3. Chromatographic and mass spectrometric analysis

Samples were analyzed using an Agilent 6530 Accurate-Mass Q-TOF coupled with a 1260 Agilent Infinity LC system equipped with a Sunfire C₁₈ column (150 x 2.1 mm ; i. d. 3.5 µm, Waters) with a flow rate of 0.25 mL/min. Full scan mass spectra were acquired in the positive-ion mode in a mass range of m/z 100 to 1200 Da, with the capillary temperature at

320°C, source voltage at 3.5 kV, and a sheath gas flow rate at 10 L/min. Capillary, fragmentor, and skimmer voltages were set at 3500 V, 175 V, and 65 V respectively. Four scan events were used: positive MS, mass range encompassing m/z 100-1200, and three data-dependent MS/MS scans of the five most intense ions from the first scan event. Three collision energies (*viz.* 30, 50, and 70 eV) were used for MS/MS data generation. Purine ($C_5H_4N_4$, m/z 121.050873 and HP-0921 (hexakis(1*H*,1*H*,3*H*-tetrafluoropropoxy)phosphazene $C_{18}H_{18}F_{24}N_3O_6P_3$, m/z 922.009798) were used as internal lock masses. Full scans were acquired at a resolution of 10 000 (m/z 922) and 4000 (m/z 121). A permanent MS/MS exclusion list criterion was established to prevent oversampling of the internal calibrant.

4.4. MZmine Data Pre-Processing, Molecular Networking, ISDB Spectral Library Search and Taxonomically-Informed Scoring Parameters.

The MS/MS data file were converted from the .d in-house Agilent data format to .mzXML thanks to the MS Convert Software, as included in ProteoWizard package (Chambers et al., 2012). All .mzXML files were further submitted to the MZmine 2v.52 workflow. The mass detection was performed with a mass detection threshold at 1.0E4. The ADAP chromatogram builder was obtained using a minimum group scan size of 4, a group intensity threshold of 1.0E4, a minimum highest intensity of 1.0E5 and m/z tolerance of 0.05 Da or 5 ppm (Myers et al., 2017). The ADAP wavelets deconvolution algorithm was applied with the following settings : S/N threshold = 10, minimum feature height = 3, coefficient/area threshold = 3, peak duration range 0.02-4.0 min, RT wavelet range 0.02-0.6. MS/MS scans were paired using a m/z tolerance range of 0.02 Da and a RT tolerance range of 1.0 min. The chromatogram was deisotoped using the isotopic peak grouper algorithm with a m/z tolerance of 0.02 Da or 10 ppm and a RT tolerance of 1.0 min. Peak alignment used the join aligner module with a m/z tolerance of 0.02 or 10 ppm (weight for m/z = 1, weight for RT = 1, absolute RT tolerance = 0.3 min). The peak list was gap-filled with the same RT and m/z range. The .mgf preclustered

data file and the corresponding .csv metadata file (for RT, areas ; and formulas integration) were exported using the dedicated built-in options. A molecular network was then created using the online workflow hosted at GNPS. The data were then clustered with MS-Cluster with a parent ion mass tolerance of 2.0 Da and a fragment ion mass tolerance of 0.5 Da to generate consensus spectra. Consensus spectra containing less than 1 spectrum were discarded. A network was then created where edges were filtered to have a minimal cosine score of 0.6 with at least six matched fragment peaks. Edges were further maintained if each of the nodes appeared in each other respective top 10 most similar nodes. When searching against GNPS libraries, matches between network spectra and library spectra required a cosine score of 0.6 and at least six matched peaks. The clustered spectra of the molecular network were further dereplicated against the ISDB, following the guidelines edicted by Allard and co-workers (Allard et al., 2016; Rutz et al., 2019). Spectral matching parameters were set as follows: tolerance = 0.005, score threshold = 0.2, Top K results = 3. A taxonomically-informed score (family=Amaryllidaceae, Genus=*Crinum*) was further applied to the in silico annotated matches. The generated molecular network were visualized using Cytoscape 3.5.1 (Shannon et al., 2003) and ChemViz 2 for structure display.

4.5. Computational details

Coordinates of the lowest-energy conformer of the different diastereoisomers differing in the configuration of C-3 and C-11 of **1** and **2** were optimized at the B3LYP/6-31 G(d) level of theory (Becke, 1993; Hehre et al., 1986; Lee et al., 1988). Chemical shifts were calculated from NMR shielding tensors using GIAO method (Ditchfield, 1974; Wolinski et al., 1990) prior to being corrected against values for the corresponding nucleus TMS, both at the same level of theory. Vibrational analysis within the harmonic approximation was performed at the same level of theory upon geometrical optimization convergence prior to characterizing local minima by the absence of imaginary frequency. Excitation energies and corresponding

rotational strengths for the first 60 electronic transitions were then calculated using the TDDFT method (Bauernschmitt et al., 1997) at the B3LYP/6-31G* level. Individual ECD spectra were computed by the summation of Gaussian functions (Stephens and Harada, 2010) using SpecDis (Bruhn et al., 2013) v1.64 software with a half-bandwidth of 0.30 eV after a bathochromic shifting of 35 nm for **1** and a sigma/gamma value of 0.16 eV and no UV correction for **2**.

4.6. Cytotoxic and antiplasmodial evaluations

See Experimental Method S59, Supporting Information (Otogo N’Nang et al., 2018).

4.7. Extraction and purification of compounds

The dried bulbs of *C. scillifolium* (1.5 kg) were milled and extracted with EtOH (3 x 3L, 24 h each, 40°C, atmospheric pressure). The EtOH extract was concentrated *in vacuo* at 40°C to afford 200 gr of dry residue that was dissolved in 6M NH₄OH. This solution was submitted to extraction with EtOAc (400 mL x 4). The EtOAc phase was extracted using a solution of sulfuric acid 2 M (200 mL x 3). This aqueous phase was alkalized using 6M NH₄OH and extracted with CH₂Cl₂ to yield 300 mg of an alkaloid extract. The dry residue was submitted to flash chromatography using a Silica 12g Grace cartridge with a gradient of CH₂Cl₂/MeOH (1:0 to 0:1) at 30 mL/min to afford five fractions based on TLC profiles. Fraction F2 (33 mg) was subjected to preparative TLC in EtOAc/MeOH (99-1) to afford asicatumine A (2.2 mg). Fraction F4 (40 mg) was fractionated by preparative HPLC separation using a gradient of MeOH-H₂O with 0.1% FA (99:1 to 6:4) to afford **1** (2.5 mg), **2** (3.3 mg), **3** (1.3 mg), isotazettinol (2.7 mg), lycorine (2.1 mg), sternbergine (2.3 mg), and 4',*O*,*N*-dimethylnorbelleadine (5.7 mg). Fraction F5 (36 mg) was submitted to preparative HPLC using the same gradient system of MeOH-H₂O with 0.1% FA (99:1 to 6:4) to yield **4** (0.5 mg), hippadine (3.2 mg), vittatine (1.6 mg), and 4'-*O*-methylnorbelleadine (1.2 mg).

4.7.1. Scillitazettine (1)

White amorphous solid; $[\alpha]_{\text{D}}^{20} + 40.0$ (c 0.1, MeOH); UV (MeOH) λ_{max} (log ϵ) 232 (4.0), 290 (3.6) nm; IR ν_{max} 3385, 2929, 1737, 1684, 1433, 1204 cm^{-1} ; ^1H and ^{13}C NMR data, see Table 1; HRESIMS m/z 360.1448 $[\text{M}+\text{H}]^+$ (calcd for $\text{C}_{19}\text{H}_{22}\text{NO}_6$, 360.14416). MS/MS spectrum was deposited in the GNPS spectral library under the identifier: CCMSLIB00005467904.

4.7.2. Scilli-N-Desmethylpretazettine (2)

White amorphous solid; $[\alpha]_{\text{D}}^{20} - 22.7$ (c 0.1, MeOH); UV (MeOH) λ_{max} (log ϵ) 228 (4.3), 262 (3.7), 310 (3.5) nm; IR ν_{max} 3385, 3224, 2927, 1739, 1684, 1433, 1205 cm^{-1} ; ^1H and ^{13}C NMR data, see Table 1; HRESIMS m/z 330.1334 $[\text{M}+\text{H}]^+$ (calcd for $\text{C}_{18}\text{H}_{20}\text{NO}_5$, 330.13360). MS/MS spectrum was deposited in the GNPS spectral library under the identifier: CCMSLIB00005467905.

4.7.3. 3-O-Acetylvittatine (3)

White amorphous solid; $[\alpha]_{\text{D}}^{20} + 28.0$ (c 0.1, MeOH); UV (MeOH), λ_{max} (log ϵ) 249 (3.5), 277 (3.1) nm; IR (ν_{max}) 3423, 1735, 1639, 1511, 1445, 1373, 1241, 1096, 1037 cm^{-1} ; ^1H and ^{13}C NMR data, see Table 1; HRESIMS m/z 314.1389 $[\text{M}+\text{H}]^+$ (calcd for $\text{C}_{18}\text{H}_{20}\text{NO}_4$, 314.13870). MS/MS spectrum was deposited in the GNPS spectral library under the identifier: CCMSLIB00005467850.

4.7.4. 4'-O,N-Dimethylnorbelladine-N-oxide (4)

Faint yellow amorphous solid; $[\alpha]_{\text{D}}^{20} 0$ (c 0.1, MeOH); UV (H_2O) λ_{max} (log ϵ) 221 (14.6), 240 (6.0), 262 (3.8), 277 (5.1) nm; IR ν_{max} 3439, 3434, 1734, 1611, 1514, 1463, 1243, 1157, 1029, 975 cm^{-1} ; ^1H and ^{13}C NMR data, see Table 3; HRESIMS m/z 304.1595 $[\text{M}+\text{H}]^+$ (calcd. for $\text{C}_{17}\text{H}_{22}\text{NO}_4$, 304.15433). MS/MS spectrum was deposited in the GNPS spectral library under the identifier: CCMSLIB00005467852.

Declaration of competing interest

The authors declare no competing financial interest.

Acknowledgements

This study was supported by sponsorship from Université Paris-Saclay and CNRS. We express our thanks to Dr Jérôme Bignon (ICSN) for performing the cytotoxicity assays. We

also thank Jean-Christophe Jullian (BioCIS) for NMR acquisition. Leo Gohrs (Alionis) is thanked for the donation of computing hardware.

References

- Abdel-Halim, O.B., Morikawa, T., Ando, S., Matsuda, H., Yoshikawa, M., 2004. New Crinine-Type Alkaloids with Inhibitory Effect on Induction of Inducible Nitric Oxide Synthase from *Crinum yemense*. *J. Nat. Prod.* 67, 1119–1124. <https://doi.org/10.1021/np030529k>
- Ali, A.A., Mesbah, M.K., Frahm, A.W., 1981. Phytochemical Investigation of *Hippeastrum vittatum* Growing in Egypt. *Planta Med.* 43, 407–409. <https://doi.org/10.1055/s-2007-971534>
- Allard, P.-M., Péresse, T., Bisson, J., Gindro, K., Marcourt, L., Pham, V.C., Roussi, F., Litaudon, M., Wolfender, J.-L., 2016. Integration of molecular networking and in-silico MS/MS fragmentation for natural products dereplication. *Anal. Chem.* 88, 3317–3323. <https://doi.org/10.1021/acs.analchem.5b04804>
- Allen, F., Greiner, R., Wishart, D., 2015. Competitive fragmentation modeling of ESI-MS/MS spectra for putative metabolite identification. *Metabolomics* 11, 98–110. <https://doi.org/10.1007/s11306-014-0676-4>
- Bauernschmitt, R., Häser, M., Treutler, O., Ahrlichs, R., 1997. Calculation of excitation energies within time-dependent density functional theory using auxiliary basis set expansions. *Chem. Phys. Lett.* 264, 573–578. [https://doi.org/10.1016/S0009-2614\(96\)01343-7](https://doi.org/10.1016/S0009-2614(96)01343-7)
- Becke, A.D., 1993. Becke's three parameter hybrid method using the LYP correlation functional. *J Chem Phys* 98, 5648–5652. <https://doi.org/10.1063/1.462066>
- Berkov, S., Osorio, E., Viladomat, F., Bastida, J., 2020. Chapter Two - Chemodiversity, chemotaxonomy and chemoecology of Amaryllidaceae alkaloids, in: Knölker, H.-J. (Ed.), *The Alkaloids: Chemistry and Biology*. Academic Press, pp. 113–185. <https://doi.org/10.1016/bs.alkal.2019.10.002>
- Bokov, D.O., Samylina, I.A., Nikolov, S.D., 2016. Amaryllidaceae alkaloids GC/MS analysis in *Galanthus woronowii* and *Galanthus nivalis* of Russian origin. *Res. J. Pharm. Biol. Chem. Sci.* 7, 1625–1629.
- Brine, N.D., Campbell, W.E., Bastida, J., Herrera, M.R., Viladomat, F., Codina, C., Smith, P.J., 2002. A dinitrogenous alkaloid from *Cyrtanthus obliquus*. *Phytochemistry* 61, 443–447. [https://doi.org/10.1016/S0031-9422\(02\)00206-6](https://doi.org/10.1016/S0031-9422(02)00206-6)
- Bruhn, T., Schaumlöffel, A., Hemberger, Y., Bringmann, G., 2013. SpecDis: Quantifying the comparison of calculated and experimental electronic circular dichroism spectra. *Chirality* 25, 243–249. <https://doi.org/10.1002/chir.22138>
- Buckingham, J., Baggaley, K.H., Roberts, A.D., Szabo, L.F., 2010. *Dictionary of Alkaloids with CD-ROM*. CRC press.
- Cabezas, F., Ramírez, A., Viladomat, F., Codina, C., Bastida, J., 2003. Alkaloids from *Eucharis amazonica* (Amaryllidaceae). *Chem Pharm Bull* 51, 315–317. <https://doi.org/10.1248/cpb.51.315>
- Campbell, W.E., Nair, J.J., Gammon, D.W., Codina, C., Bastida, J., Viladomat, F., Smith, P.J., Albrecht, C.F., 2000. Bioactive alkaloids from *Brunsvigia radulosa*. *Phytochemistry* 53, 587–591. [https://doi.org/10.1016/S0031-9422\(99\)00575-0](https://doi.org/10.1016/S0031-9422(99)00575-0)
- Cedron, J.C., Gutiérrez, D., Flores, N., Ravelo, Á.G., Estévez-Braun, A., 2012. Synthesis and antimalarial activity of new haemanthamine-type derivatives. *Bioorg. Med. Chem.* 20, 5464–5472. <https://doi.org/10.1016/j.bmc.2012.07.036>
- Chambers, M.C., Maclean, B., Burke, R., Amodei, D., Ruderman, D.L., Neumann, S., Gatto, L., Fischer, B., Pratt, B., Egertson, J., Hoff, K., Kessner, D., Tasman, N., Shulman, N., Frewen, B., Baker, T.A., Brusniak, M.-Y., Paulse, C., Creasy, D., Flashner, L., Kani, K., Moulding, C., Seymour, S.L.,

- Nuwaysir, L.M., Lefebvre, B., Kuhlmann, F., Roark, J., Rainer, P., Detlev, S., Hemenway, T., Huhmer, A., Langridge, J., Connolly, B., Chadick, T., Holly, K., Eckels, J., Deutsch, E.W., Moritz, R.L., Katz, J.E., Agus, D.B., MacCoss, M., Tabb, D.L., Mallick, P., 2012. A cross-platform toolkit for mass spectrometry and proteomics. *Nat. Biotechnol.* 30, 918–920. <https://doi.org/10.1038/nbt.2377>
- Ditchfield, R., 1974. Self-consistent perturbation theory of diamagnetism: I. A gauge-invariant LCAO method for NMR chemical shifts. *Mol. Phys.* 27, 789–807. <https://doi.org/10.1080/00268977400100711>
- Dudek, M.J., Ponder, J.W., 1995. Accurate modeling of the intramolecular electrostatic energy of proteins. *J. Comput. Chem.* 16, 791–816. <https://doi.org/10.1002/jcc.540160702>
- Dumont, P., Ingrassia, L., Rouzeau, S., Ribaucour, F., Thomas, S., Roland, I., Darro, F., Lefranc, F., Kiss, R., 2007. The Amaryllidaceae Isocarbostryril Narciclasine Induces Apoptosis By Activation of the Death Receptor and/or Mitochondrial Pathways in Cancer Cells But Not in Normal Fibroblasts. *Neoplasia* 9, 766–776. <https://doi.org/10.1593/neo.07535>
- Eichhorn, J., Takada, T., Kita, Y., Zenk, M.H., 1998. Biosynthesis of the amaryllidaceae alkaloid Galanthamine. *Phytochemistry* 49, 1037–1047. [https://doi.org/10.1016/S0031-9422\(97\)01024-8](https://doi.org/10.1016/S0031-9422(97)01024-8)
- Elgorashi, E.E., Drewes, S.E., Van Staden, J., 1999. Alkaloids from *Crinum bulbispermum*. *Phytochemistry* 52, 533–536. [https://doi.org/10.1016/S0031-9422\(99\)00255-1](https://doi.org/10.1016/S0031-9422(99)00255-1)
- Evidente, A., Cicala, M.R., Giudicianni, I., Randazzo, G., Riccio, R., 1983. ¹H and ¹³C NMR analysis of lycorine and alpha-dihydrolycorine. *Phytochemistry* 22, 581–584. [https://doi.org/10.1016/0031-9422\(83\)83051-9](https://doi.org/10.1016/0031-9422(83)83051-9)
- Evidente, A., Iasiello, I., Randazzo, G., 1984. Isolation of Sternbergine, a New Alkaloid From Bulbs of *Sternbergia lutea*. *J. Nat. Prod.* 47, 1003–1008. <https://doi.org/10.1021/np50036a017>
- Evidente, A., Kornienko, A., 2009. Anticancer evaluation of structurally diverse Amaryllidaceae alkaloids and their synthetic derivatives. *Phytochem. Rev.* 8, 449–459. <https://doi.org/10.1007/s11101-008-9119-z>
- Fennell, C.W., Van Staden, J., 2001. *Crinum* species in traditional and modern medicine. *J. Ethnopharmacol.* 78, 15–26. [https://doi.org/10.1016/S0378-8741\(01\)00305-1](https://doi.org/10.1016/S0378-8741(01)00305-1)
- Fox Ramos, A.E., Alcover, C., Evanno, L., Maciuk, A., Litaudon, M., Duplais, C., Bernadat, G., Gallard, J.-F., Jullian, J.-C., Mouray, E., Grellier, P., Loiseau, P.M., Pomel, S., Poupon, E., Champy, P., Beniddir, M.A., 2017. Revisiting Previously Investigated Plants: A Molecular Networking-Based Study of *Geissospermum laeve*. *J. Nat. Prod.* 80, 1007–1014. <https://doi.org/10.1021/acs.jnatprod.6b01013>
- Fox Ramos, A.E., Evanno, L., Poupon, E., Champy, P., Beniddir, M.A., 2019a. Natural products targeting strategies involving molecular networking: different manners, one goal. *Nat. Prod. Rep.* 36, 960–980. <https://doi.org/10.1039/C9NP00006B>
- Fox Ramos, A.E., Le Pogam, P., Fox Alcover, C., Otogo N’Nang, E., Cauchie, G., Hazni, H., Awang, K., Bréard, D., Echavarren, A.M., Frédéric, M., Gaslonde, T., Girardot, M., Grougnet, R., Kirillova, M.S., Kritsanida, M., Lémus, C., Le Ray, A.-M., Lewin, G., Litaudon, M., Mambu, L., Michel, S., Miloserdov, F.M., Muratore, M.E., Richomme-Peniguel, P., Roussi, F., Evanno, L., Poupon, E., Champy, P., Beniddir, M.A., 2019b. Collected mass spectrometry data on monoterpene indole alkaloids from natural product chemistry research. *Sci. Data* 6. <https://doi.org/10.1038/s41597-019-0028-3>
- Frahm, A.W., Ali, A.A., Ramadan, M.A., 1985. ¹³C nuclear magnetic resonance spectra of amaryllidaceae alkaloids. I—alkaloids with the crinane skeleton. *Magn. Reson. Chem.* 23, 804–808. <https://doi.org/10.1002/mrc.1260231004>
- Halgren, T.A., 1995. Merck molecular force field. I. Basis, form, scope, parameterization, and performance of MMFF94. *J. Comput. Chem.* 17, 490–519. [https://doi.org/10.1002/\(SICI\)1096-987X\(199604\)17:5/6<490::AID-JCC1>3.0.CO;2-P](https://doi.org/10.1002/(SICI)1096-987X(199604)17:5/6<490::AID-JCC1>3.0.CO;2-P)
- Hehre, W.J., Radom, L., Schleyer, P.V.R., Pople, J.A., 1986. *Ab initio* Molecular Orbital Theory. Wiley.

- Herrera, M.R., Machocho, A.K., Brun, R., Viladomat, F., Codina, C., Bastida, J., 2001. Crinane and Lycorane Type Alkaloids from *Zephyranthes citrina*. *Planta Med.* 67, 191–193. <https://doi.org/10.1055/s-2001-11495>
- Hotchandani, T., Desgagne-Penix, I., 2017. Heterocyclic Amaryllidaceae alkaloids: biosynthesis and pharmacological applications. *Curr. Top. Med. Chem.* 17, 418–427.
- Jin, Z., Yao, G., 2019. Amaryllidaceae and *Sceletium* alkaloids. *Nat. Prod. Rep.* 10.1039/C8NP00055G. <https://doi.org/10.1039/C8NP00055G>
- Kobayashi, S., Kihara, M., Shingu, T., Shingu, K., 1980. Transformation of tazettine to pretazettine. *Chem. Pharm. Bull. (Tokyo)* 28, 2924–2932. <https://doi.org/10.1248/cpb.28.2924>
- Kolossváry, I., Guida, W.C., 1999. Low-Mode Conformational Search Elucidated: Application to C₃₉H₈₀ and Flexible Docking of 9-Deazaguanine Inhibitors into PNP. *J. Comput. Chem.* 20, 14. [https://doi.org/10.1002/\(SICI\)1096-987X\(19991130\)20:15<1671::AID-JCC7>3.0.CO;2-Y](https://doi.org/10.1002/(SICI)1096-987X(19991130)20:15<1671::AID-JCC7>3.0.CO;2-Y)
- Kong, Y., Ponder, J.W., 1997. Calculation of the reaction field due to off-center point multipoles. *J. Chem. Phys.* 107, 481–492. <https://doi.org/10.1063/1.474409>
- Koua Kadio Brou, D., Effen Kouakou, E., Kouakou, S.L., Droucoula, G.C., Yapi Houphouet, F., 2017a. Evaluation of the analgesic activity of the aqueous and hydroethanolic extract from *Crinum scillifolium* Bulbs (Amaryllidaceae). *Int. J. Biochem. Res. Rev.* 20, 1–7.
- Koua Kadio Brou, D., Irié-N'guessan Amenan, G., Effen Kouakou, E., Kouakou, S.L., Ayoman, T.L.D., Tetchi, A.F., Houphouët Boigny, F., 2018. Evaluation of Anti-inflammatory Activity of *Crinum scillifolium* Extracts in Wistar Rats. *Int. J. Biochem. Biophys.* 6, 77–82.
- Koua Kadio Brou, D., N'Tamon, A.D., Okpekon Aboua, T., Kouakou, S.L., Yapi Houphouet, F., 2017b. Evaluation of the Anticonvulsant Activity of the Aqueous Extract of *Crinum scillifolium* Bulbs (Amaryllidaceae) In Experimental Animals. *IOSR J. Pharm. Biol. Sci.* 12, 35–39.
- Kundrot, C.E., Ponder, J.W., Richards, F.M., 1991. Algorithms for calculating excluded volume and its derivatives as a function of molecular conformation and their use in energy minimization. *J. Comput. Chem.* 12, 402–409. <https://doi.org/10.1002/jcc.540120314>
- Lee, C., Yang, W., Parr, R.G., 1988. Development of the Colle-Salvetti correlation-energy formula into a functional of the electron density. *Phys. Rev. B* 37, 785–789. <https://doi.org/10.1103/PhysRevB.37.785>
- López, S., Bastida, J., Viladomat, F., Codina, C., 2002. Acetylcholinesterase inhibitory activity of some Amaryllidaceae alkaloids and *Narcissus* extracts. *Life Sci.* 71, 2521–2529. [https://doi.org/10.1016/S0024-3205\(02\)02034-9](https://doi.org/10.1016/S0024-3205(02)02034-9)
- Masi, M., Frolova, L.V., Yu, X., Mathieu, V., Cimmino, A., De Carvalho, A., Kiss, R., Rogelj, S., Pertsemliadis, A., Kornienko, A., Evidente, A., 2015. Jonquiline, a new pretazettine-type alkaloid isolated from *Narcissus jonquilla quail*, with activity against drug-resistant cancer. *Fitoterapia* 102, 41–48. <https://doi.org/10.1016/j.fitote.2015.01.009>
- Myers, O.D., Sumner, S.J., Li, S., Barnes, S., Du, X., 2017. One Step Forward for Reducing False Positive and False Negative Compound Identifications from Mass Spectrometry Metabolomics Data: New Algorithms for Constructing Extracted Ion Chromatograms and Detecting Chromatographic Peaks. *Anal. Chem.* 89, 8696–8703. <https://doi.org/10.1021/acs.analchem.7b00947>
- Nair, J., Campbell, W., Brun, R., Viladomat, F., Codina, C., Bastida, J., 2005. Alkaloids from *Nerine filifolia*. *Phytochemistry* 66, 373–382. <https://doi.org/10.1016/j.phytochem.2004.12.009>
- Nair, van Staden, 2019a. Antiplasmodial Studies Within the Plant Family Amaryllidaceae. *Nat. Prod. Commun.* 14, 1934578X19872931. <https://doi.org/10.1177/1934578X19872931>
- Nair, van Staden, 2019b. Antiplasmodial lycorane alkaloid principles of the plant family Amaryllidaceae. *Planta Med.* 85, 637–647. <https://doi.org/10.1055/a-0880-5414>
- Nair, van Staden, 2019c. Antiplasmodial constituents in the minor alkaloid groups of the Amaryllidaceae. *South Afr. J. Bot.* 126, 362–370. <https://doi.org/10.1016/j.sajb.2019.06.012>
- Nothias, L.F., Petras, D., Schmid, R., Dührkop, K., Rainer, J., Sarvepalli, A., Protsyuk, I., Ernst, M., Tsugawa, H., Fleischauer, M., 2019. Feature-based Molecular Networking in the GNPS Analysis Environment. *bioRxiv* 812404.

- Olivier-Jimenez, D., Chollet-Krugler, M., Rondeau, D., Beniddir, M.A., Ferron, S., Delhay, T., Allard, P.-M., Wolfender, J.-L., Sipman, H.J., Lücking, R., Boustie, J., Le Pogam, P., 2019. A database of high-resolution MS/MS spectra for lichen metabolites. *Sci. Data* 6, 1–11. <https://doi.org/10.1038/s41597-019-0305-1>
- Otogo N’Nang, E., Bernadat, G., Mouray, E., Kumulungui, B., Grellier, P., Poupon, E., Champy, P., Beniddir, M.A., 2018. Theionbrunonines A and B: Dimeric Vobasine Alkaloids Tethered by a Thioether Bridge from *Mostuea brunonis*. *Org. Lett.* 20, 6596–6600. <https://doi.org/10.1021/acs.orglett.8b02961>
- Pabuçcuoglu, V., Richomme, P., Gözler, T., Kivçak, B., Freyer, A.J., Shamma, M., 1989. Four New Crinine-Type Alkaloids from *Sternbergia* Species. *J. Nat. Prod.* 52, 785–791. <https://doi.org/10.1021/np50064a020>
- Pham, L., Gründemann, E., Wagner, J., Bartoszek, M., Döpke, W., 1999. Two novel Amaryllidaceae alkaloids from *Hippeastrum equestre* Herb.: 3-O-demethyltazettine and egonine. *Phytochemistry* 51, 327–332. [https://doi.org/10.1016/S0031-9422\(98\)00743-2](https://doi.org/10.1016/S0031-9422(98)00743-2)
- Pilar Vazquez Tato, M., Castedo, L., Riguera, R., 1988. New alkaloids from *Pancreatium maritimum* L. *Heterocycles* 27, 2833–2838. <https://doi.org/10.3987/COM-88-4694>
- Refaat, J., Kamel, M.S., Ramadan, M.A., Ali, A.A., 2013. *Crinum*; an endless source of bioactive principles: a review. part v. biological profile. *Int. J. Pharm. Sci. Res.* 4, 1239.
- Refaat, J., Kamel, M.S., Ramadan, M.A., Ali, A.A., 2012a. *Crinum*; an endless source of bioactive principles: a review. Part 1-Crinum alkaloids: lycorine-type alkaloids. *Int. J. Pharm. Sci. Res.* 3, 1883.
- Refaat, J., Kamel, M.S., Ramadan, M.A., Ali, A.A., 2012b. *Crinum*; an endless source of bioactive principles: a review. Part III; crinum alkaloids: Belladine-, galanthamine-, lycorenine-, tazettine-type alkaloids and other minor types. *Int. J. Pharm. Sci. Res.* 3, 3630.
- Rutz, A., Dounoue-Kubo, M., Ollivier, S., Bisson, J., Bagheri, M., Saesong, T., Ebrahimi, S.N., Ingkaninan, K., Wolfender, J.-L., Allard, P.-M., 2019. Taxonomically Informed Scoring Enhances Confidence in Natural Products Annotation. *Front. Plant Sci.* 10, 1329. <https://doi.org/10.3389/fpls.2019.01329>
- Shannon, P., Markiel, A., Ozier, O., Baliga, N.S., Wang, J.T., Ramage, D., Amin, N., Schwikowski, B., Ideker, T., 2003. Cytoscape: a software environment for integrated models of biomolecular interaction networks. *Genome Res.* 13, 2498–2504. <https://doi.org/10.1101/gr.1239303>
- Singh, A., Desgagné-Penix, I., 2017. Transcriptome and metabolome profiling of *Narcissus pseudonarcissus* ‘King Alfred’ reveal components of Amaryllidaceae alkaloid metabolism. *Sci. Rep.* 7, 17356. <https://doi.org/10.1038/s41598-017-17724-0>
- Stephens, P.J., Harada, N., 2010. ECD cotton effect approximated by the Gaussian curve and other methods. *Chirality* 22, 229–233. <https://doi.org/10.1002/chir.20733>
- Suau, R., Gómez, A.I., Rico, R., Tato, M.V., Castedo, L., Riguera, R., 1988. Alkaloid N-oxides of Amaryllidaceae. *Phytochemistry* 27, 3285–3287. [https://doi.org/10.1016/0031-9422\(88\)80044-X](https://doi.org/10.1016/0031-9422(88)80044-X)
- Sun, Q., Shen, Y.-H., Tian, J.-M., Tang, J., Su, J., Liu, R.-H., Li, H.-L., Xu, X.-K., Zhang, W.-D., 2009. Chemical Constituents of *Crinum asiaticum* L. var. *sinicum* Baker and Their Cytotoxic Activities. *Chem. Biodivers.* 6, 1751–1757. <https://doi.org/10.1002/cbdv.200800273>
- Tallini, L., Andrade, J., Kaiser, M., Viladomat, F., Nair, J., Zuanazzi, J., Bastida, J., 2017. Alkaloid constituents of the Amaryllidaceae plant *Amaryllis belladonna* L. *Molecules* 22, 1437. <https://doi.org/10.3390/molecules22091437>
- Thomsen, T., Kewitz, H., 1990. Selective inhibition of human acetylcholinesterase by galanthamine in vitro and in vivo. *Life Sci.* 46, 1553–1558. [https://doi.org/10.1016/0024-3205\(90\)90429-U](https://doi.org/10.1016/0024-3205(90)90429-U)
- Torras-Claveria, L., Berkov, S., Jáuregui, O., Caujapé, J., Viladomat, F., Codina, C., Bastida, J., 2010. Metabolic profiling of bioactive *Pancreatium canariense* extracts by GC-MS. *Phytochem. Anal.* 21, 80–88. <https://doi.org/10.1002/pca.1158>

- Ünver, N., Noyan, S., Gözler, T., Önür, M.A., Gözler, B., Hesse, M., 1999. Three New Tazettine-Type Alkaloids from *Galanthus gracilis* and *Galanthus plicatus* Subsp. *byzantinus*. *Planta Med.* 65, 347–350. <https://doi.org/10.1055/s-1999-14062>
- Wagner, J., Pham, H.L., Döpke, W., 1996. Alkaloids from *Hippeastrum equestre* Herb.—5. Circular dichroism studies. *Tetrahedron* 52, 6591–6600. [https://doi.org/10.1016/0040-4020\(96\)00297-9](https://doi.org/10.1016/0040-4020(96)00297-9)
- Wang, H.-Y., Qu, S.-M., Wang, Y., Wang, H.-T., 2018. Cytotoxic and anti-inflammatory active plicamine alkaloids from *Zephyranthes grandiflora*. *Fitoterapia* 130, 163–168. <https://doi.org/10.1016/j.fitote.2018.08.029>
- Wang, M., Carver, J.J., Phelan, V.V., Sanchez, L.M., Garg, N., Peng, Y., Nguyen, D.D., Watrous, J., Kaponov, C.A., Luzzatto-Knaan, T., 2016. Sharing and community curation of mass spectrometry data with Global Natural Products Social Molecular Networking. *Nat. Biotechnol.* 34, 828. <https://doi.org/10.1038/nbt.3597>
- Wolinski, K., Hinton, J.F., Pulay, P., 1990. Efficient implementation of the gauge-independent atomic orbital method for NMR chemical shift calculations. *J. Am. Chem. Soc.* 112, 8251–8260. <https://doi.org/10.1021/ja00179a005>
- Zetta, L., Gatti, G., Fuganti, C., 1973. ^{13}C nuclear magnetic resonance spectra of amaryllidaceae alkaloids. *J. Chem. Soc. Perkin Trans. 2* 1180–1184. <https://doi.org/10.1039/P29730001180>
- Zhan, G., Zhou, J., Liu, R., Liu, T., Guo, G., Wang, J., Xiang, M., Xue, Y., Luo, Z., Zhang, Y., 2016. Galanthamine, plicamine, and secoplicamine alkaloids from *Zephyranthes candida* and their anti-acetylcholinesterase and anti-inflammatory activities. *J. Nat. Prod.* 79, 760–766. <https://doi.org/10.1021/acs.jnatprod.5b00681>
- Zou, G., Puig-Basagoiti, F., Zhang, B., Qing, M., Chen, L., Pankiewicz, K.W., Felczak, K., Yuan, Z., Shi, P.-Y., 2009. A single-amino acid substitution in West Nile virus 2K peptide between NS4A and NS4B confers resistance to lycorine, a flavivirus inhibitor. *Virology* 384, 242–252. <https://doi.org/10.1016/j.virol.2008.11.003>

GRAPHICAL ABSTRACT

